VIZOR: Virtually Zero Margin Adaptive RF for Ultra Low Power Wireless Communication

Rajarajan Senguttuvan, Shreyas Sen and Abhijit Chatterjee
Georgia Institute of Technology, Atlanta, GA, USA.
{rajs, shreyas.sen, chat @ece.gatech.edu}

Abstract[1]

Modern wireless transceiver systems are often over-designed to meet the requirements of low bit error rate values at high data rates under worst-case channel operating conditions (interference, noise, multi-path effects). This results in circuits being designed with "sufficient" margins leading to lower efficiency and high power consumption. In this paper, we develop an adaptive power management strategy for RF systems that optimally trades-off power vs. performance for the RF front-end to maintain operation at or below a specified maximum bit error rate (BER) across temporally changing operating conditions. As the communication channel degrades, more power is consumed by the RF front end and vice versa. Since the maximum bit-error rate specification is not violated, minimum voice or video quality through the wireless channel is always guaranteed.

1. Introduction

With the emergence of wireless handsets as multi-purpose communications as well as computing devices, the issue of handset power consumption and heat dissipation is dominating future designs. Though several low-power design techniques have been developed for digital systems [1]-[3], relatively fewer techniques have been proposed for radio frequency (RF) systems. Techniques for power minimization in RF circuits include bias current reuse [5], functional combination [6], controlled positive feedback [7], and sub threshold biasing [8]. An energy scalable RF transmitter with increased power efficiency was presented in [9].

Existing wireless power management schemes [9]-[11] modulate the data rate (radio-link control) based on the certain channel quality metrics derived from the analysis of received training symbols. Training symbols are short bit sequences that are transmitted prior to the data to ascertain the channel, and to calibrate the receiver for current channel conditions. For each data rate, the circuit is then tuned to a fixed supply or bias voltage. The issue with these approaches is that acceptable baseband (demodulated) signal fidelity levels to achieve specified bit-error rates need to account for worst case estimates of process variability and thermal effects in the RF front-end, and channel conditions corresponding to different data rates of transmission. Operating the RF front-end with such pre-set worst case performance margins causes power-inefficient operation of the wireless device. However, by using *closed-loop feedback control*, significant battery energy consumption can be saved when the device is operating under favourable channel conditions. Moreover, while power/performance enhancement techniques for RF transmitters have been investigated, no comparable work exists for RF receivers. In the following sections, the key idea of the paper is first described followed by a detailed discussion of the proposed power reduction approach for a wireless receiver.

2. Key Idea

The key idea of the work presented in this paper is to exploit built-in design margins in wireless systems across temporally changing channel conditions to save power. For this purpose, a suitable adaptation metric that quantifies the cumulative sum of the quality of transmission (this is well controlled at the radio base station), the channel quality degradation and the quality of signal reception, is chosen. The *adaptation metric* is computed by the baseband signal processor in real-time (online). When this adaptation metric has a "high" value (high fidelity of the received signal) the quality of signal processing in the RF front end (i.e. its

[1] This work was funded in part by NSF ITR award CCR-0325555 and GSRC/FCRP 2003-DT-660.

performance) can be degraded intentionally by reducing its supply and bias voltages dynamically to save power while maintaining a specified maximum bit-error-rate (BER).

In the proposed approach, the wireless front-end always strives to operate at the lowest power consumption levels (lower performance) for any specified modulation. The use of such a feedback control technique to adapt to dynamically changing air channel conditions saves significant amount of power whenever the channel quality is not worst-case (while satisfying the BER condition). A corollary of this approach is that as channel degrades, with the use of appropriate feedback control techniques for controlling the supply and bias voltages, the same receiver will automatically consume more power in an effort to make up for decreased channel quality. The above mentioned concepts are demonstrated using an OFDM receiver front end as the test vehicle.

3. Wireless Receiver System Development

Circuit-level implementations of the LNA and mixer are realized and ADS simulations are performed for various supply and bias settings to cahracterize their performance. The data from these simulations is then used to develop behavioral models, which are used for system-level study of the proposed approach. The behavioral modeling of key components in the OFDM receiver module and channel is presented.

3.1. LNA and Mixer circuit implementations

A wideband LNA is designed in CMOS 0.18u technology. A common gate (CG) input stage provides good input matching over a wide range, the common source (CS) intermediate stage provides the required gain, and the class A output stage provides good signal swing. The operating range of the designed LNA is from 2-7 GHz, and the gain is observed to be 16 dB at 2.4GHz for a nominal supply voltage of 1.8V and bias of 0.8V. The LNA has NF of about 3dB, and the total DC power consumption of the LNA is about 25.6mW.

For the mixer, a double-balanced Gilbert cell architecture was chosen. A balun is used for single-to-double ended conversion. The mixer provides a gain of 11.8 dB, NF of 8 dB. The operating range of the mixer is from 2-7GHz, and the power consumption of 6.6mW at a nominal supply voltage of 1.8V and bias of 0.8V.

The power consumption of the LNA and mixer decreases with the lowering of supply and bias voltages, but trades-offs with gain, non-linearity and NF specifications. This, in turn affects the system-level performance. For this work, the set of supply (V_{ddL}, V_{ddM}) and bias (V_{bL}, V_{bM}) voltages of LNA/mixer that is used for adaptation is given below.

V_{ddL}, V_{ddM}	[1.8 1.6 1.4 1.2 1.0]
V_{bL}, V_{bM}	[0.8 0.7 0.6 0.5]

The modeling of the LNA and mixer is realized through a non-linear transfer function of the type

$$y(t) = \alpha_0 + \alpha_1 x(t) + \alpha_2 x^2(t) + \alpha_3 x^3(t) + \alpha_4 x^4(t) + \alpha_5 x^5(t) \quad \textbf{(1)}$$

where α_0 is the DC offset, α_1 is the small signal gain, and α_2, α_3, α_4, α_5 are non-linearity coefficients. The coefficients define the linear (gain) and non-linear (harmonics and inter-modulation terms) effects of the amplifier. Transistor-level simulation data for the LNA and mixer obtained from the Agilent ADS tool is used to extract the coefficients in Equation (1). The NF is factored-in through addition of white noise to the output signal. For the mixer, in addition to the non-linear transfer function implementation, the frequency mixing operation is realized by a simple multiplication operation as given in Equation (2).

$$Y(t) = C \times x_1(t) \times x_2(t) \quad \textbf{(2)}$$

where, C represents conversion gain of the mixer.

The choice of supply and bias voltages of the LNA and mixer constitute a total of 400 different settings. Behavioral parameters of the RF front-end are extracted for each of these 400 configurations for use in the simulation study. It should be noted here that many of these 400 configurations are not optimal from a power consumption standpoint. Therefore, The set of configurations are pruned down to a limited set of optimal values using a multi-dimensional optimization approach in the design phase. The reduced set of supply and bias voltages are used to dynamically configure the RF front-end during run time for minimizing power across changing environmental conditions using an optimal control law.

3.2. Baseband functionality

At the transmit end of the OFDM baseband, input serial data stream is formatted into the word size required for transmission, e.g. 2 bits/word for quadrature phase shift keying (QPSK) or 4 bits/word for quadrature amplitude modulation (16-QAM). The data is converted to parallel format and sent to a inverse fast fourier transform (IFFT) block. The IFFT block converts the parallel modulated data to the

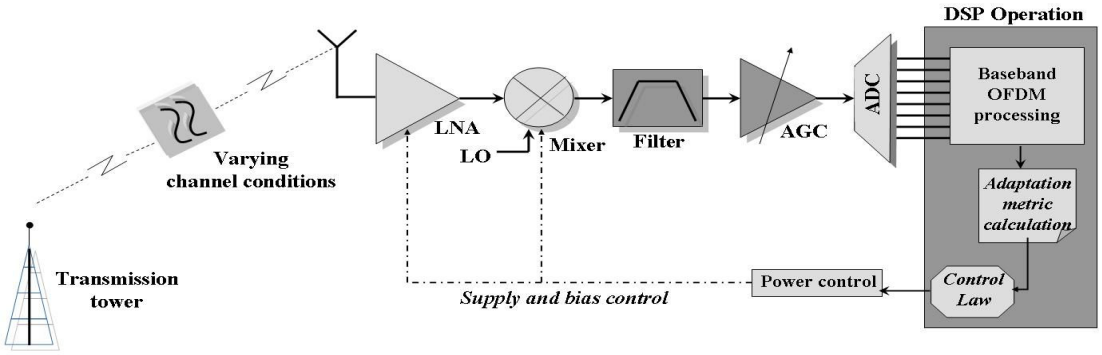

Figure 1 Feedback-driven wireless receiver system

corresponding time waveform (symbol) that is transmitted. The receiver portion performs a reverse operation on the received signal (serial-to-parallel conversion, FFT) to obtain data bits.

3.3. Channel modeling

The effect of the channel includes the sum contribution of the air-antenna interface effect at the transmitter and receiver, respectively, and the effect of the physical medium (air) between the transmit and receive antennas.

(1) Propagation loss and noise addition are modeled as a simple attenuation of the received signal followed by addition of white noise to the received signal.

(2) The multipath and fading effect are modeled using an FIR filter. The length of the FIR filter determines the maximum delay spread in the channel.

(3) Interference is modeled as a combination of adjacent channel interference and microwave interference. Adjacent channel interferer is modeled as an OFDM signal in a neighboring band. Emissions from this band affect the signal in the band of interest (2.4GHz). The adjacent channel interferer is given by

$$i\_adj(t) = f(A(t), f_c(t))_{OFDM} \quad \textbf{(3)}$$

where A(t) is the time varying amplitude and fc(t) is the time varying frequency. The microwave interferer is modeled as an AM-FM source that allows the characterization of frequency wander based on the work presented in [13]. AM-FM modulation is employed on a time-varying sinusoidal signal to generate the microwave interferer. The frequency of the microwave interferer is given by

$$f_d(t) = f_0 + f_w \sin\left(\frac{2\pi t}{T_w}\right) \quad \textbf{(4)}$$

where f_o and f_w are initial interferer frequency and the maximum frequency wander, respectively, and T_w is frequency wander period. For this work, fo is 2.412GHz, f_w is 20MHz, and T_w is chosen as 20ms.

4. Choosing a Suitable Adaptation Metric

The choice of the adaptation metric is driven by the requirement that it should encompass the sum effect of non-idealities in RF front-end/analog blocks, channel effects and noise etc. In other words, the adaptation metric must provide the best indication of the system performance under all possible environmental conditions. The performance of a communication system is usually quantified in terms of the BER of the system. BER, as the name suggests, gives the rate at which errors occur during communication. Typical values for wireless systems are in the order of 10^{-3}-10^{-4}. Measuring the BER of a system typically incurs a long time as several thousand bits are transmitted and received.

A metric (system specification) that can easily measured in DSP using less time, and which strongly correlates to the system BER specification is highly desirable. The choice of EVM as an adaptation metric in a tunable word length OFDM receiver was explored in [15]. EVM, like BER is an at-speed specification of a wireless system i.e. it is measured during the actual operation of the device. It is computed as

$$EVM = \sqrt{\frac{1}{N}\frac{\sum_{1}^{N}\|y_i - x_i\|^2}{\|y_{\max}\|^2}} \quad \textbf{(5)}$$

where, y_i and x_i are the received and transmitted complex modulated data *(I+jQ)*, y_{max} is the outermost data point in the constellation, and *N* is the number of data points used for computation. From the above equation, EVM quantifies the difference between the transmitted and received modulated data. EVM can be

easily calculated for each data frame of the received signal. System-level simulations were performed to ascertain and establish a relationship between the EVM and BER specifications. Figure 2 plots the EVM and BER for a wireless system under different channel conditions and system non-idealities. Two different modulation schemes used in practice – QPSK and 16-QAM were employed for evaluation purposes and about 10^5 bits were transmitted and received.

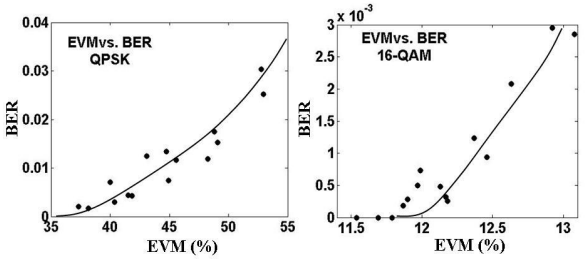

Figure 2 EVM vs. BER relation: System-level simulations

The different values of EVM and BER are obtained by perturbing channel conditions and the RF front-end non-linearities. From the plots it is observed that in general an increase in EVM is associated with an increase in BER, and vice versa. A relationship between the two specifications can therefore be established. An upper bound on the BER specification can then be translated into an upper bound on the EVM. For example, if BER bound is set at 5e-4, the corresponding mean EVM bound for the QPSK and 16-QAM cases can be approximated to about 35% and 12%, respectively. Moreover, it should be noted that the EVM specification is determined by random processes in the channel and the device among other factors. A simulation was therefore performed to analyze the repeatability. The 3σ variation of the EVM value is accounted for in setting the *threshold value* and a *guard band* around it for any desired BER value.

5. Proposed Approach for Minimum Power Operation of the Receiver

In this section, the proposed approach for minimum power operation is described from a system-level perspective. Figure 3 illustrates the proposed approach that enables the operation of the wireless device at minimum power consumption levels for any environmental condition while satisfying the pre-set threshold metric. The system under consideration consists of the receiver RF front-end and the baseband processing module, which continuously evaluates the performance metric for received OFDM symbols, and operates the RF front-end close to the error threshold through feedback control.

Figure 3 shows the flow chart of required iterations during the design and characterization phase as well as the control scheme during the run time operation of the device. During the design and characterization phase, first a set of tunable control 'knobs' are identified that trade-off the device performance with power consumption. For our purpose, the supply and bias voltages of the LNA (V_{ddL}, V_{bL}) and the mixer (V_{ddM}, V_{bM}) are used as the control parameters. A finite set of channel conditions that adequately span the range 'good' to 'bad' are modeled. The different channels are obtained by perturbing the different channel parameters (noise, multipath components, and interference sources). For each of these channel conditions, the optimal set of tuning parameters are computed through co-optimization for the power and EVM metrics as described below. The computed optimal set for different channel conditions define an optimal locus of tuning parameter values corresponding to the lowest power consumption for maximum allowed EVM. During run time operation, the control law running in the DSP operates the system along this optimal locus for varying channel conditions.

5.1. Power and EVM Optimization

A simple heuristic co-optimization procedure is used to compute the optimal set of tuning parameters (voltages) for each channel condition, and is performed as follows. Initially, with the device operating under nominal voltage condition: V_{ddL}= 1.8V, V_{bL}= 0.8V, V_{ddM}= 1.8V, V_{bM}= 0.8V the following matrix (*M*) is calculated through simulations.

$$M = \begin{bmatrix} \frac{\partial p}{\partial V_{ddL}} & \frac{\partial p}{\partial V_{bL}} & \frac{\partial p}{\partial V_{ddM}} & \frac{\partial p}{\partial V_{bM}} \\ \frac{\partial EVM}{\partial V_{ddL}} & \frac{\partial EVM}{\partial V_{bL}} & \frac{\partial EVM}{\partial V_{ddM}} & \frac{\partial EVM}{\partial V_{bM}} \\ \frac{\partial p}{\partial EVM_{ddL}} & \frac{\partial p}{\partial EVM_{bL}} & \frac{\partial p}{\partial EVM_{ddM}} & \frac{\partial p}{\partial EVM_{bM}} \end{bmatrix}$$

For example, $\frac{\partial p}{\partial V_{ddL}}$ and $\frac{\partial EVM}{\partial V_{ddL}}$ denotes the change in power consumption and EVM metric for a unit change in supply voltage of the LNA (V_{ddL}), and likewise for other entries in matrix *M*. The third row

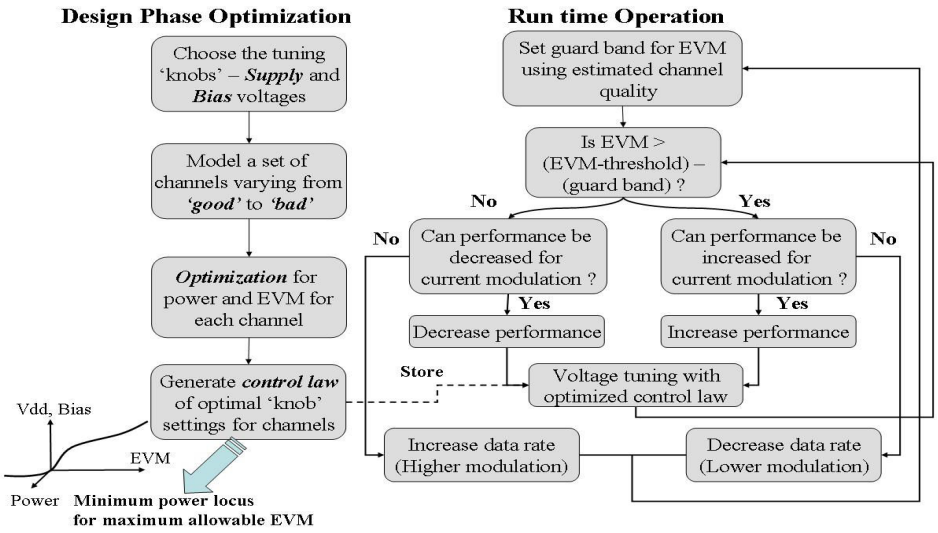

Figure 3 Proposed feedback-driven approach for low-power operation

of the matrix is obtained through a simple ratio of these two quantities. It is to be noted then that each entity in the third row of matrix *M* provides an estimate of the change in power consumption of the circuit for a unit change in the EVM metric. The tuning parameter for each iteration is then chosen by selecting the maximum of the four entities in the third row. This allows us to tune the voltage parameter that produces *the maximum reduction in power consumption for the least increase in EVM*. Once a particular voltage parameter is selected, it is scaled down to generate a new set and matrix *M* is recomputed, and the procedure is repeated. The iteration steps continue until the EVM threshold condition is violated or all possibilities are exhausted. Thus, an optimal voltage set (V_{ddL}, V_{bL}, V_{ddM}, and V_{bM}) is obtained for each channel condition. These values are then stored in a look-up table (LUT) in the DSP for adaptation during the online operation of the wireless device.

5.2. Run-time operation of the device

During run operation, the voltages are continuously scaled down to reduce power consumption of the device for every data rate (modulation). With the scaling down of the voltages, the system-level performance metric (EVM) degrades. This is allowed to continue until the EVM is within certain pre-defined threshold value. Guard band for the EVM threshold is set based on the channel quality. For example, a poor channel would have a larger guard band and vice versa. After this, the performance (supply and bias voltages) of the RF front-end is increased or decreased for the current data rate depending on the computed EVM. The voltages are scaled up or down based on the optimized control law stored in the lookup table. The device power consumption, thus hovers around the lowest possible value for which received signal quality meets the required specification. This scheme achieves significant power savings by operating the system at the lowest possible power for all channel conditions using closed loop feedback control.

6. Simulation Results and Inferences

Simulations were performed on the receiver system to obtain the optimal voltage set for different channels. The system was first simulated for QPSK modulation, and then for 16-QAM modulation. A set of 12 different channels *(Channel 1(best) – Channel 12 (worst))* was modeled for study purposes. The optimal voltages obtained from the simulations for various channels are plotted in Figure 4. The received QPSK and 16-QAM constellations for nominal voltage operation, and at optimal voltage values (EVM metric close to the threshold) are shown in Figure 5.

As observed from Figure 4, the computed optimal voltage set varies between the nominal (0.8V, 1.8V, 0.8V, 1.8V) to the lowest possible values (0.5V, 1.0V, 0.5V, 1.0V) over the different channel conditions . It is seen that for a majority of the channel conditions, the receiver operates at the lower than nominal voltage values allowing for significant savings in device power consumption. It is also observed that the optimal

voltage values and the associated power consumption is lower for QPSK-modulated signals compared to 16-QAM. This is due to the tighter requirements on the signal quality and SNR for a 16-QAM signal (higher data rates).

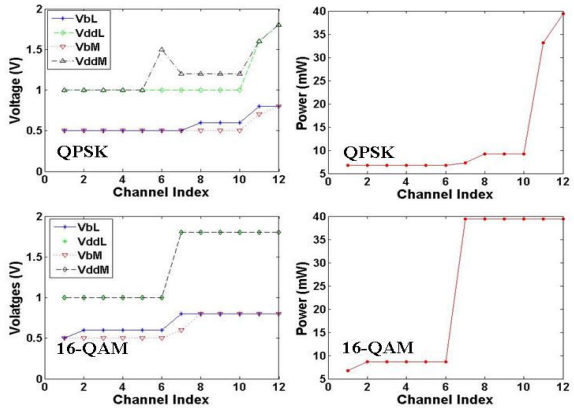

Figure 4 Optimal supply and bias voltages and power consumption for different channel conditions

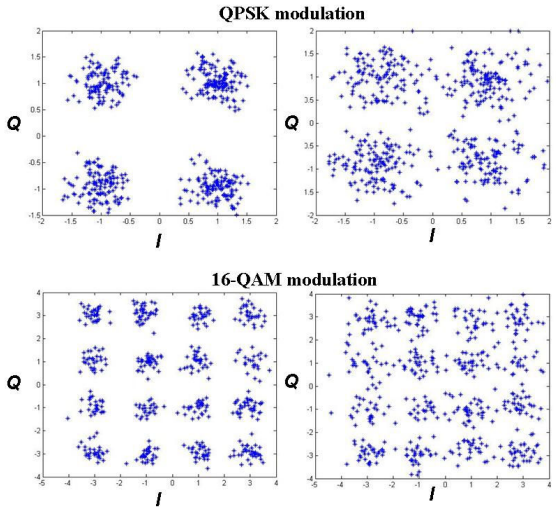

Figure 5 Constellation degradation with voltage scaling

The plots shown in Figure 5 highlight the key advantage of the proposed approach – exploitation of the design margins to operate the device at the threshold. In the absence of feed-back driven adaptation, the receiver system always operates at nominal voltage levels (power = 40mW), whereas in the proposed approach the power consumption tends towards 40mW only for certain channels (only *Channel 12* for QPSK modulation). For good channels, QPSK modulation requirements are met at RF front-end power levels of just 6.6mW (16.5% of the nominal power).

In present-day wireless systems, the data rate (modulation) is dynamically changed by the higher-level protocol depending on channel conditions. For example, the modulation is changed from QPSK to 16-QAM (higher data rates) if the channel conditions are good. Due to the shift in modulation, the power savings that can be obtained is reduced (due to tighter requirements of 16-QAM) in favor of higher transmission rates. However, the feedback-driven control then ensures that the device operation is optimal for 16-QAM modulation. Thus, the proposed approach enables the receiver operation at lowest *(virtually zero margin)* power consumption levels for all modulations under temporally varying environmental conditions.

6.1. Effect of process variations

Process variability causes the performance metrics of manufactured devices to vary from the nominal values. The effect of process variability on the power consumption in the proposed adaptation scheme is shown in Figure 6. A set of 50 perturbed instances of the LNA and mixer were simulated in ADS and the corresponding behavioral parameters were extracted for simulations in MATLAB. The adaptive run time feedback control was then implemented for the set of 50 devices, for 4 different channel conditions. Figure 6 plots the variation in the optimal power consumption metric among the 50 perturbed instances for different channels.

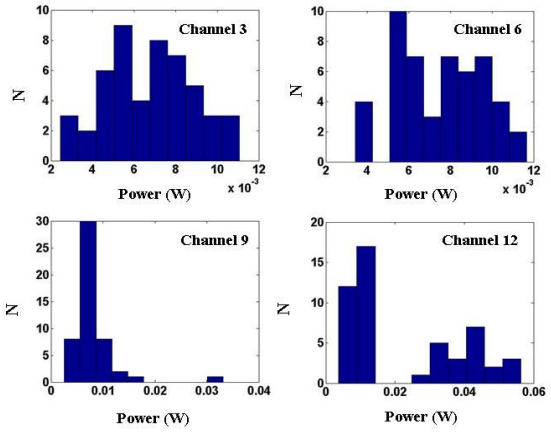

Figure 6 Effect of process variations on the receiver power consumption for different channel conditions

The feedback control scheme operates the perturbed devices along the optimal locus for each channel based on the control law. Though the optimal control law (supply and bias control) stored in the LUT

is obtained for a nominal device during characterization phase, it is still effective in operating different process-skewed devices at reduced power consumption levels. This is feasible due to the feedback-driven control mechanism that is employed to tune the tuning knobs of the device. Thus for all the 50 perturbed devices, the voltages are regulated such that the operation is close to the error boundary. The amount of power savings for each device depends on its process spread and its correlation to the optimal locus obtained for a nominal device.

7. Conclusions

A scheme for dynamic feedback-driven adaptation of wireless devices for minimum power operation is proposed in this paper. The adaptation framework is implemented on a RF receiver front-end, and the feasibility is demonstrated through circuit and system-level simulations. The proposed approach takes into account the effect of the entire receive chain in a wireless communication system including circuit non-idealities and environmental factors. The adaptive control scheme operates the system at the lowest possible power consumption levels for any data rate (modulation) under all channel conditions. System-level simulation results demonstrate the effectiveness of the proposed approach.

8. References

[1] S. Lee, S. Das, T. Pham, T. Austin, D. Blaauw and T. Mudge, "Reducing Pipeline Energy Demands with Local DVS and Dynamic Retiming," Proceedings of the ISLPED'04, Aug 2004, pp: 319-324.

[2] D. Ernst, N. S. Kim, S. Das, S. Pant, R. Rao, T. Pham, C. Ziesler, D. Blaauw, T. Austin, K. Flautner and T. Mudge, "Razor: A Low-Power Pipeline Based on Circuit-Level Timing Speculation," Proceedings of the 36th International Symposium on Microarchitecture (MICRO-36'03), pp: 7 – 18.

[3] D. Ernst, S. Das, S. Lee, D. Blaauw, T. Austin, T. Mudge, N. S. Kim, K. Flautner, "RAZOR: Circuit-Level Correction Of Timing Errors For Low-Power Operation," IEEE Micro, Vol. 24, Issue 6, Nov-Dec 2004 pp:10 – 20.

[4] Q. Huang, .F. Piazza, P. Orsatti and T. Ohguro, "The Impact of Scaling Down to Deep Submicron on CMOS RF Circuits," IEEE Journal of Solid-State Circuits, Vol. 33, No. 7, July 1998, pp. 1023-1036.

[5] A. N. Karanicolas, "A 2.7-V 900-MHz CMOS LNA and Mixer," IEEE Journal of Solid-State Circuits, Vol. 31, No. 12, December 1996, pp. 1939-1944.

[6] C. Y. Wu and H. S. Kao, "A 2-V Low-Power CMOS Direct-Conversion Quadrature Modulator With Integrated Quadrature Voltage-Controlled Oscillator and RF Amplifier for GHz RF Transmitter Applications," IEEE Transactions On Circuits And Systems—II: Analog And Digital Signal Processing, Vol. 49, No. 2, February 2002, pp. 123-134.

[7] T. Kawamura, M. Suzuki and H. Ichino, "An Extremely Low-power Bipolar Current-mode 1/0 Circuit for Multi-Gbit/s Interfaces," Proceedings of 1994 Symposium on VLSl, June 1994, pp: 31-32.

[8] B. G. Perumana, S. Chakraborty, C. H. Lee,and J. Laskar, "A Fully Monolithic 260-_W, 1-GHz Subthreshold Low Noise Amplifier," IEEE Microwave And Wireless Components Letters, Vol. 15, No. 6, June 2005, pp. 428-430.

[9] Debaillie, B. Bougard, B., Lenoir, G., Vandersteen G., Catthoor, F., "Energy-scalable OFDM transmitter design and control", 43rd IEEE Design Automation Conference, july 24-28, pp. 536-541.

[10] Tasic, A., Serdjin, W.A., Long, J.R., "Adaptive multi-standard ciruits and systems for wireless communications", IEEE Circuits and Systems Magazine, Vol 6., Issue 1., pp. 29-37.

[11] Abidi, A., Pottie, G.J., Kaiser, W.J., "Power-conscious design of wireless circuits and systems", Proceedings of the IEEE, vol 88,Issue 10, Oct 2000, pp. 1528-1545.

[12] G. Gielen, W. Dehaene, "Analog and digital circuit design in 65 nm CMOS: end of the road?," Proceedings of the Design, Automation and Test in Europe Conference and Exhibition (DATE'05), 2005 pp. 37 – 42.

[13] Zhao, Y., Agee, B.G., Reed, J.H., "Simulation and measurement of microwave oven leakage for 802.11 WLAN interference management", Microwave, Antenna, Propagation and EMC Technologies for Wireless Communications, vol 2, Aug 8-12, 2005, pp.1580-1583.

[14] Sahu, B., Rincon-Mora, G.A., "A high-efficiency linear RF power amplifier with a power-tracking dynamically adaptive buck-boost supply," IEEE Transactions on Microwave Theory and Techniques, Volume 52, Issue 1, Part 1, Jan. 2004 Page(s):112 – 120.

[15] Yoshizawa, S., Miyanaga, Y., "Tunable wordlength architecture for a low power wireless OFDM demodulator", IEICE Transaction Fundamentals, Vol E89-A, No. 10, October 2006.